

General Disclaimer

One or more of the Following Statements may affect this Document

- This document has been reproduced from the best copy furnished by the organizational source. It is being released in the interest of making available as much information as possible.
- This document may contain data, which exceeds the sheet parameters. It was furnished in this condition by the organizational source and is the best copy available.
- This document may contain tone-on-tone or color graphs, charts and/or pictures, which have been reproduced in black and white.
- This document is paginated as submitted by the original source.
- Portions of this document are not fully legible due to the historical nature of some of the material. However, it is the best reproduction available from the original submission.

(NASA-TM-85119) SPECTRAL ANALYSIS OF
MAGNETOHYDRODYNAMIC FLUCTUATIONS NEAR
INTERPLANETARY SHOCKS (NASA) 43 p
A03/MF A01

N84-13044

CSSL 03B

G3/90

Unclas
42562



Technical Memorandum 85119

**SPECTRAL ANALYSIS OF
MAGNETOHYDRODYNAMIC
FLUCTUATIONS
NEAR INTERPLANETARY SHOCKS**

**Adolfo F. Viñas
Melvyn L. Goldstein
and
Mario H. Acuña**



NOVEMBER 1983

National Aeronautics and
Space Administration

Goddard Space Flight Center
Greenbelt, Maryland 20771

SPECTRAL ANALYSIS OF MAGNETOHYDRODYNAMIC FLUCTUATIONS

NEAR INTERPLANETARY SHOCKS

Adolfo F. Viñas

Melvyn L. Goldstein

and

Mario H. Acuña

Laboratory for Extraterrestrial Physics
NASA/Goddard Space Flight Center
Greenbelt, MD 20771

Submitted to: Journal of Geophysical Research

Abstract

Evidence for two types of relatively large amplitude MHD waves upstream and downstream of quasi-parallel forward and reverse interplanetary shocks is presented. The first mode is an Alfvén wave with frequencies (in the spacecraft frame) in the range of 0.025 - 0.07 Hz. This is a left-hand polarized mode and propagates within a few degrees of the ambient magnetic field. The second is a fast MHD mode with frequencies in the range of 0.025 - 0.17 Hz, right-hand polarization and propagating along the magnetic field. These waves are detected principally in association with quasi-parallel shocks ($\theta_{Bn} < 45^\circ$). The Alfvén waves are found to have plasma rest frame frequencies in the range of 1.1 - 6.3 mHz with wavelengths in the order of $4.8 \times 10^8 - 2.7 \times 10^9$ cm. Similarly, the fast MHD modes have rest frame frequencies in the range 1.6 - 26 mHz with typical wavelengths about $2.19 \times 10^8 - 9.51 \times 10^8$ cm. The magnetic field power spectrum in the vicinity of these interplanetary shocks is much steeper than $f^{-5/3}$ at high frequencies. The observed spectra have a high frequency dependence of $f^{-2.5}$ to f^{-4} . A peculiar feature of the fast mode identification in one event is the large correlation observed between $|\vec{B}|$ and proton density ρ for field aligned propagation. This appears to be a nonlinear effect, second order in the wave amplitude. An interpretation of these observations is given in terms of the electromagnetic ion beam instability. Both resonant and nonresonant interactions need to be considered to account for the polarization and spectral content of the observed fluctuations.

1. Introduction

Recent experimental observations and theoretical modeling have pointed out the importance of plasma waves upstream of interplanetary shocks in understanding the structure of collisionless shocks and the origin of energetic particles often observed in association with shocks [Tsurutani et al., 1983; Acuña et al., 1981]. These observations have detected two types of upstream waves. A high frequency whistler mode with frequencies as measured in the spacecraft frame between 0.2 and 2 Hz and a low frequency fast MHD mode near 50 mHz. Both wave modes are observed to have circular or elliptical right-hand polarization (in the plasma frame), and propagate within 15° of the mean magnetic field direction. Similar observations of wave phenomena upstream of planetary bow shocks, including observations of left-hand waves, have been discussed by Barnes [1970], Fairfield [1969, 1974], Russell et al. [1971], Hoppe and Russell [1983], Smith et al. [1983], Goldstein et al. [1983] and Smith et al. [1984].

In this paper, we present preliminary results of an investigation of magnetic fluctuations seen upstream of two interplanetary shocks. The spectral analysis includes calculation of the normalized reduced magnetic helicity spectrum $\sigma_m(k)$, the normalized reduced cross helicity spectrum $\sigma_c(k)$, and the Alfvén ratio $r_A(k)$ as discussed by Matthaeus and Goldstein [1982]. Minimum variance methods are used to compute wave polarization as a function of frequency. The Taylor "frozen-in-flow" hypothesis is assumed [Taylor, 1935, 1938; Matthaeus and Goldstein, 1982] to convert frequencies to wave-vectors. Some of the basic properties of the waves including the probable mode of propagation in association with both quasi-parallel forward and reverse shocks are described. A comparison with previous results on the

generation of waves at interplanetary and planetary shocks is presented.

Section 2 contains a discussion of the spectral techniques. Section 3 contains a discussion of the linear theory of the electromagnetic ion beam instability which we utilize to explain the excitation of the observed fluctuations. The results are discussed and summarized in section 4.

2. Observations

The Voyager (GSFC) magnetometer and (MIT) plasma teams have compiled a list of interplanetary shocks from launch (October 1977) to 1980 for time intervals when simultaneous observations are available. The plasma parameters were determined from either moment calculations or from a Gaussian-fit procedure as discussed by Bridge et al. [1977]. We used only the moment calculations which were computed from data sampled every 12 s during the time periods discussed in this paper. The magnetometer aboard Voyagers 1 and 2 has a much higher time resolution [see Behannon et al., 1977]. Magnetic power spectra and magnetic helicity spectra were computed using 1.92 second average magnetic field data. Consequently, these spectra extend to higher frequencies than the plasma data. Shock normals were calculated from the plasma-magnetic field data using a single spacecraft method of shock normal estimation developed by Lepping and Argentiero [1971] and improved by Acuña. The time periods of interest in this paper are 0800 - 1000 UT on January 29 and 1850 - 2000 UT on February 3, 1978.

January 29, 1978 -- Upstream

Figure 1 shows a plot of the magnitude and components of the magnetic

field and plasma bulk velocity for January 29 in the RTN (radial, tangential and normal) heliocentric coordinate system together with the proton number density and temperature. Note the presence of a quasi-parallel reverse shock at about 0918:17 UT. The shock normal components for this event are $\hat{n} = (-0.92, -0.35, -0.17)$ and the angle between the normal and the average upstream magnetic field is about 11° . The shock structure and its properties for this event has been recently investigated by Scudder et al. [1983]. For the spectral analysis calculation we have selected the upstream and downstream regions (excluding the shock itself) which correspond to the subintervals from 0919:10 to 1000 UT and 0800:45 to 0914:39 UT, respectively.

For the upstream subinterval the components of the average magnetic field are $(-1.13, -0.56, -0.46)$ nT, and the average solar wind speed is 366 km/s. The fluctuations in all the components and in the magnitude are rather large, typically $(\delta B)_{\text{rms}}/| \langle B_0 \rangle | \approx 0.40$. As usual when data is available from only a single spacecraft, only reduced (one dimensional) spectra can be determined [Batchelor, 1970]. We use the fast Fourier transform technique with 26 degrees of freedom to compute these spectra. Details of our analysis techniques can be found in Matthaeus and Goldstein [1982]. In Figure 2 we show the magnetic field power spectrum corresponding to this subinterval. Note that it possesses an f^{-4} power-law dependence at high frequencies, which differs substantially from the typical ambient solar wind behavior of $f^{-5/3}$ [Jokipii and Coleman, 1968; Matthaeus and Goldstein, 1982]. The bulge in the spectrum centered about $f \approx 8 \times 10^{-3}$ Hz reflects the presence of quasi-monochromatic fluctuations in the upstream region of this shock.

The normalized reduced magnetic helicity spectrum $\sigma_m(k) = |k|H_m(k)/E_b(k)$ is plotted in Figure 3a. $E_b(k)$ and $H_m(k)$ are the reduced spectra of magnetic energy and magnetic helicity, respectively. $E_b(k)$ is the trace of the

spectral matrix $S_{ij}^r(k)$ defined from [cf. Matthaeus and Goldstein, 1982]:

$$S_{ij}^r(k_1) = \int dk_2 dk_3 S_{ij}^r(k_1, k_2, k_3)$$

The magnetic helicity is defined by

$$H_m \equiv \int d^3x \vec{A} \cdot \vec{B} = \int d^3k H_m(\vec{k})$$

The reduced helicity spectrum $H_m(k)$ is computed from [Matthaeus and Goldstein, 1982]:

$$H_m(k) = 2 \operatorname{Im} S_{23}^r(k)/k$$

where the components "23" correspond to "TN". The total magnetic helicity $H_m = \int dk H_m(k)$, is a measure of the lack of mirror symmetry of the magnetic field and determines its topological handedness or "knottedness" [Moffatt, 1978; Matthaeus and Goldstein, 1982]. The magnetic helicity spectrum will be positive for left-hand topological structures and negative for right-hand topological structures. The sign of the magnetic helicity is directly related to the sense of polarization as defined in optics [Jackson, 1962]. A discussion of the relationship between the magnetic helicity and the polarization can be found in Smith et al. [1983]. An important fundamental property of the magnetic helicity is that because it is a Galilean invariant, once determined in the spacecraft frame it is also known in the plasma frame (subject to the constraint that one is dealing with MHD phenomena). Therefore the sense of polarization determined from it corresponds to the polarization in the plasma frame. Note in Figure 3a that the magnetic helicity increases with frequency

becoming positive ($\sigma_m \sim 0.8$) for frequencies in the range of 0.025 - 0.07 Hz, indicating the presence of left-hand helices in the magnetic field. This magnetic helicity spectrum is distinctly different from the randomly oscillating spectra normally observed in the solar wind far from planetary and interplanetary shocks [Matthaeus and Goldstein, 1982; Smith et al., 1983].

An eigenvalue (minimum variance) analysis of this interval was performed in which the spectral matrix was rotated into an eigenvalue coordinate system at each mode. This yields the degree of polarization and ellipticity of the fluctuations as a function of frequency. The smallest eigenvalue is associated with the direction of minimum variance of the fluctuations for each Fourier mode. This is the direction of $\pm \vec{k}$ under the assumption that decomposition into plane waves is appropriate.

Figure 3b-d shows the results of this analysis. In Figure 3b we plot the degree of polarization D , the ellipticity ϵ and the cosine of the angle between \vec{k} and \vec{B}_0 . The calculation imposes the requirement that \vec{k} has a positive projection in the +R direction. The normalized magnetic helicity and the degree of polarization track each other very well. Also note that the ellipticity is large when both the magnetic helicity and the degree of polarization are large, implying nearly circular polarization. Therefore, subject to the condition that the fluctuations have phase speed less than the solar wind speed, the waves must be left-hand circularly polarized in the plasma frame [Smith et al. 1983]. In addition, the cosine of the angle between \vec{k} and \vec{B}_0 , $\cos\theta$, is large for frequencies from 0.001 to 0.1 Hz. Thus these fluctuations should not be compressive. Because the rest frame polarization is left-hand, these fluctuations are probably Alfvén waves propagating nearly parallel (or anti-parallel) to the ambient magnetic field.

We have checked that these waves are noncompressive by correlating the

density measurements ρ with the magnetic field magnitude $|\vec{B}|$. Alfvén waves (and parallel propagating fast mode waves) should show little if any correlation between $|\vec{B}|$ and ρ if $\theta \approx 0$. This correlation is shown in Figure 4b using 14 degrees of freedom for frequencies from 0.025 to 0.04 Hz, which is the only range that overlaps the magnetic spectrum. Note that the magnetic field magnitude and plasma density correlation appears to give almost no correlation since the peaks in this frequency range tend to oscillate about zero. However this should be interpreted with some caution because the fluctuations have very small amplitude and the correlation may not be well resolved.

The eigenvalue analysis can only determine the wave phase velocity direction to within a sign. However, this ambiguity can be resolved by calculating the cross-helicity spectrum. The reduced normalized cross-helicity spectrum is defined as $\sigma_c(k) \approx 2H_c(k)/E(k)$ where $E(k)$ and $H_c(k)$ are the spectral decomposition of the total energy spectrum (magnetic plus kinetic) and the cross-helicity spectrum, respectively. The cross helicity measures the correlation between the velocity and magnetic fluctuations and is defined by:

$$H_c = \int d^3x \vec{v} \cdot \vec{b} = \int d^3k H_c(\vec{k})$$

where $b = \delta B / \sqrt{4\pi\rho}$. The total energy in these Alfvén velocity units is

$$E = \int d^3x (v^2 + b^2) = \int d^3k [E_v(\vec{k}) + E_b(\vec{k})]$$

When $\sigma_c(k)$ is near ± 1 , Alfvénic fluctuations are present in the data. Thus, if the magnetic field and the velocity fluctuations are in the same direction ($\sigma_c = +1$) the wave energy is propagating antiparallel to the mean magnetic

field. If they are in the opposite sense ($\sigma_c = -1$), then the wave energy is propagating parallel to \vec{B}_0 . Figure 4a shows the normalized cross-helicity $\sigma_c(k)$ spectrum as a function of frequency. The spectrum is negative and quite large ($\sigma_c \approx -0.95$) for frequencies in the range of 0.025 to 0.04 Hz. The negative sign indicates that the fluctuations are propagating parallel to the average magnetic field which is directed away of the shock and toward the Sun. The fact that the cross-helicity is large also tends to confirm that the fluctuations are Alfvénic and not whistler waves because the plasma data used only included protons.

Further confirmation that these fluctuations are MHD and not whistler waves is indicated by the Alfvén ratio $r_A(k) = E_v(k)/E_b(k)$ plotted in Figure 4c. This quantity measures the degree of equipartition between the magnetic energy and the kinetic energy. Kraichnan [1965] predicted that in fully developed MHD turbulence the two should be approximately equal at wave numbers large compared to those characterizing the energy-containing scales. Note that for whistler waves, r_A should be nearly zero because the plasma measurements we use do not include the electron data [Matthaeus and Goldstein, 1982; Goldstein et al., 1983].

January 29 — Downstream

A similar analysis has been performed in the downstream interval (from 0800:45 to 0914:39 UT) of the January 29 quasi-parallel reverse shock. In this interval the components of the average magnetic field are (-1.47, -0.76, -1.07) nT and the average solar wind speed is 337 km/s. The typical amplitude of these fluctuations is again sizeable, $(\delta B)_{rms}/|\langle B_0 \rangle| = 0.42$. The magnetic field power spectrum (Figure 5) has an $f^{-2.5}$ power-law dependence at high freq-

uencies and it contains a peak centered about $f \approx 0.013$ Hz indicating the presence of quasi-monochromatic fluctuations in the downstream region.

Figures 6a-d show the calculations of the magnetic helicity spectrum σ_m , the degree of polarization D , the ellipticity ϵ and the cosine of the angle θ between \vec{k} and \vec{B}_0 . Note that near $f \approx 0.013$ Hz the magnetic helicity is positive ($\sigma_m \approx 0.3$) indicating left-hand helices. Similarly the degree of polarization and ellipticity yield $D \approx 0.6$ and $\epsilon \approx 0.5$ respectively. The fluctuations near $f \approx 0.013$ Hz appear to be elliptically polarized Alfvén waves propagating parallel to the magnetic field as indicated in Figure 6d.

In Figure 7a-c the calculation of the cross-helicity spectrum, the $|\vec{B}|-\rho$ correlation and the Alfvén ratio r_A are shown. Because the cross-helicity is negative and large ($\sigma_c \approx -0.8$), the fluctuations are propagating parallel to the magnetic field (which in this case is toward the shock and the Sun). The magnitude of the cross-helicity again suggests that these are Alfvénic fluctuations and not whistlers. Because the rest frame polarization is left-hand ($\sigma_m > 0$), we infer that the fluctuations are Alfvén modes propagating quasi-parallel to the ambient magnetic field. Figure 7b shows the $|\vec{B}|-\rho$ correlation using 14 degrees of freedom for frequencies near $f \approx 0.013$ Hz which are the only range that overlaps with the magnetic spectrum. Note that this calculation appears to indicate almost no correlation since the peaks in this frequency range tend to fluctuate about zero. The Alfvén ratio r_A for this interval is plotted in Figure 7c. At all frequencies r_A is near one as expected for MHD fluctuations.

Although the peak at $f \approx 0.013$ Hz is the most prominent (see Figure 5), there is also a relatively broad enhancement at higher frequencies. From Figures 6a-d we see that σ_m becomes negative (right hand helices) at higher frequencies. The maximum value is reached at about $f \approx 0.14$ Hz where $\sigma_m \approx$

-0.6. The good agreement between σ_m , D and ϵ for frequencies about 0.05 - 0.2 Hz suggests that the downstream region may contain both Alfvén and fast mode waves. However we are unable to determine with certainty if these right-hand waves are indeed fast MHD modes because the Nyquist frequency of the plasma data is well below the frequency range of these waves.

February 3, 1978

Another example of low frequency waves upstream of an interplanetary quasi-parallel forward shock is presented in Figure 8. Here we show a forward shock forming at about 1928 UT on February 3, 1978. We have selected the upstream region (excluding the shock) which corresponds to the subinterval from 1850 to 1926 UT for the spectral analysis. During this subinterval the components of the mean magnetic field are (-1.60, 1.56, -1.16) nT and the average solar wind speed is 399 km/s. The fluctuations in this example have about the same magnitude as before; $(\delta B)_{\text{rms}}/|<B_0>| = 0.26$. The shock normal components for this event are $\hat{n} = (-0.69, 0.62, -0.366)$ and the angle between the normal and the average upstream magnetic field is about 7.57° .

In Figure 9 we show the magnetic power spectrum for this event which has an $f^{-3.5}$ power-law dependence at high frequencies. A bulge in the power spectrum centered about $f \approx 0.035$ Hz indicates the presence of quasi-monochromatic fluctuations. $\sigma_m(k)$, D , ϵ , and $\cos\theta$ are plotted in Figure 10a-d. The magnetic helicity decreases with frequency becoming negative ($\sigma_m \approx -0.5$) in the range 0.025 - 0.17 Hz, indicating the presence of right-hand helices. Also, D and $\sigma_m(k)$ track each other well. The ellipticity as shown in Figure 10c is also large ($\epsilon \approx 0.9$). Thus, these fluctuations are nearly circularly polarized.

Because the rest frame polarization indicates right-hand polarization, these fluctuations are probably fast MHD modes propagating almost exactly parallel to the ambient magnetic field (cf. Figure 10d). To determine the sign of the direction of propagation, we evaluated the cross helicity (Figure 11a). From the positive values in this frequency range, we conclude that these fluctuations are propagating away from the shock (and the Sun). Protons streaming away from the shock can thus be in resonance with these waves. The large values ($r_A \approx 1$) of the Alfvén ratio in Figure 11c lend further confirmation that these fluctuations are MHD and not whistler.

However, there is an interesting difficulty with this interpretation in terms of linear wave modes. Note that the $|\vec{B}|-\rho$ correlation (Figure 11b) is relatively large (≈ 0.6). This is rather surprising because if θ is very small, the Alfvén and the fast MHD branches become degenerate to lowest order, and, on the basis of linear theory, little compression should be present.

We have investigated this phenomenon more fully. In Figures 12a and 12b, the power spectrum of the density fluctuations and the power in $|B|$ are plotted. Both spectra show an enhancement between 0.025 and 0.04 Hz, confirming the high correlation noted in Fig. 11b. However, the amount of power in the spectrum of $|B|$ is much lower than in the components (Fig. 9). The observed correlation between $|B|$ and ρ , therefore, may be a rather high order effect.

It is well known that the degeneracy of the Alfvén mode and the fast mode is broken if one treats the fast mode to second order in wave amplitude. Barnes and Hollweg [1974] studied an aspect of this problem. If one assumes that to lowest order the MHD waves have linear polarization, then to second order the relationship between density fluctuations and transverse magnetic field fluctuations for nearly parallel propagation is given by:

$$\frac{\delta\rho}{\rho_0} = \frac{(\delta\vec{B}_\perp)^2 - \langle\delta\vec{B}_\perp^2\rangle}{2(B_0^2 - 4\pi\gamma P_0)} \quad (1)$$

where $\delta\rho$ is the density perturbation in the wave, ρ_0 is the mean density, $\delta\vec{B}_\perp$ is the amplitude of the transverse magnetic wave field, $\langle\rangle$ represents a temporal average, and P_0 is the mean pressure.

The difficulty with applying (1) to our observations is that the observed wave is nearly purely circularly polarized. For circularly polarized fluctuations, there is no second order correction for parallel propagation and the right hand side of (1) vanishes. Another related interpretation of the data is that the $|B|-\rho$ correlation represents not a high order correction to the MHD mode amplitude, but rather evidence for mode coupling between the MHD wave thought of as a pump and another "daughter" wave via a modulational instability. The theory of modulational instabilities has been developed by Lashmore-Davies [1976], Derby [1978], Goldstein [1978], Sakai and Sonnerup [1983], among many others. If one treats the pump wave as being circularly polarized, and assumes parallel propagation, then the wave equation relating density to magnetic field is

$$\frac{\partial^2\delta\rho}{\partial t^2} - c_s^2 \frac{\partial^2\delta\rho}{\partial z^2} = \frac{1}{4\pi} \frac{\partial^2}{\partial z^2} (\vec{B}_\perp \cdot \delta\vec{B}_\perp) + \frac{1}{8\pi} \frac{\partial^2}{\partial z^2} (\delta\vec{B}_\perp \cdot \delta\vec{B}_\perp) \quad (2)$$

If we now assume that the daughter wave $\delta\vec{B}_\perp$ is also linearly polarized, the last term on the right-hand-side of (2) is zero. An analysis similar to that which led to (1) shows that the relationship between $\delta\rho$, \vec{B}_\perp and $\delta\vec{B}_\perp$ is

$$\frac{\delta\rho}{\rho_0} = \frac{(2\vec{B}_\perp \delta\vec{B}_\perp + \delta\vec{B}_\perp^2)}{4(B_0^2 - 4\pi\gamma_p P_0)} \quad (3)$$

We have estimated the extent to which (3) is satisfied for this data interval. The quantity $\delta\rho$ is estimated from the power spectrum of the density by integrating the power in the frequency range 0.025 - 0.04 Hz. One can estimate $(\vec{B}_\perp \delta\vec{B}_\perp)$ by rotating the magnetic field data into the mean-field coordinate system. The components transverse to the mean are then easily extracted and $\delta\vec{B}_\perp(t) = [\vec{B}_\perp(t) - \langle\vec{B}_\perp\rangle]$.

We take $\gamma_p = 5/3$, $P_0 = NKT$ and $T = 8.26 \times 10^4$ °K, which allows both sides of (3) to be estimated independently. The result is that $\delta\rho/\rho_0 = 4.7 \times 10^{-2}$, while the right-hand-side of (3) is 8.4×10^{-3} . The fact that the two differ by a factor of six suggests that either additional physical processes are important or that our estimates of the quantities in (3) are inadequate. The latter is certainly possible in that, first of all, the interacting waves are not monochromatic as was assumed in (3); although the power spectrum is peaked near 0.035Hz, it is certainly not a delta function (see Figure 12). Secondly, the assumption that the magnetic and density fluctuations are linearly polarized can be only approximately valid. Finally, (3) was derived under the assumption that the pressure is isotropic, but the presence of pressure anisotropies may significantly modify the analysis (see Hollweg, 1971).

3. Linear Instability Analysis

At planetary shocks similar waves as those described in the previous section have been investigated by Barnes [1970], Gary et al. [1981], Sentman

et al. [1981], Lee [1982], and Goldstein et al. [1983], among others. The principal result of these papers is that such waves may be generated by either resonant particle interactions excited by the protons reflected (or accelerated) at planetary shocks, or by a non-resonant interaction of the waves with a "diffuse" ion population which arises from pitch-angle scattering of the reflected component. In this section, we present a similar analysis and discussion of the generation mechanism for our observations.

In this paper we limit our discussion to the field aligned electromagnetic ion beam instability. A more complete analysis, including oblique propagation and a comprehensive search of the Voyager plasma data for evidence of the existence of the required ion distributions will be deferred to a later paper. Our model consists of a background electron-proton plasma that is uniform and infinite through which an ion beam is streaming. We assume that the frequency ω of the fluctuations (in the plasma frame) is smaller than the ion gyrofrequency Ω_i . The drift velocities of both the background ion and the ion beam (V_{oi} and V_{ob} , respectively) are also directed along the magnetic field, but the electron drift velocity is zero ($V_{oe} = 0$). The medium is assumed to be charge neutral ($n_e = n_i + n_b$) and to have zero current ($n_i V_{oi} + n_b V_{ob} = 0$) where n_e , n_i and n_b are the number densities of the background electrons, ions and the beam components, respectively. The zeroth order distribution for the j th component is a drifting bi-Maxwellian of the form

$$f_j^{(0)}(v_{\parallel}, v_{\perp}) = \frac{1}{\pi^{3/2} \alpha_{\perp j}^2 \alpha_{\parallel j}} \exp\left[-\frac{v_{\perp}^2}{\alpha_{\perp j}^2} - \frac{(v_{\parallel} - V_{oj})^2}{\alpha_{\parallel j}^2}\right] \quad (4)$$

where $\alpha_{\perp j}$ and $\alpha_{\parallel j}$ are the perpendicular and parallel thermal velocities defined as

$$\alpha_{\parallel j} = (2k_B T_{\parallel j} / m_j)^{1/2}, \quad \alpha_{\perp j} = (2k_B T_{\perp j} / m_j)^{1/2}$$

k_B is the Boltzmann constant, m_j is the mass of the j th species and $T_{\parallel j}$ and $T_{\perp j}$ are the parallel and perpendicular temperatures of the j th species respectively.

The dispersion relation for parallel propagating low frequency electromagnetic waves is [see, for example, Montgomery and Tidman (1964)]:

$$\begin{pmatrix} D_R \\ D_L \end{pmatrix} = \omega^2 - k_{\parallel}^2 c^2 + \sum_j \omega_{pj}^2 \int dv_{\parallel} \int \frac{v_{\perp}^2 \chi_j(v_{\parallel}, v_{\perp})}{\omega - k_{\parallel} v_{\parallel} \pm \Omega_j} dv_{\perp} = 0 \quad (5)$$

and

$$\chi_j(v_{\parallel}, v_{\perp}) = (\omega - k_{\parallel} v_{\parallel}) \frac{\partial f_j^{(o)}}{\partial v_{\perp}} + k_{\parallel} v_{\perp} \frac{\partial f_j^{(o)}}{\partial v_{\parallel}}$$

where ω is the (complex) wave frequency, $\omega_{pj} = (4\pi n_j q_j^2 / m_j)^{1/2}$ is the plasma frequency of the j th species, c is the velocity of light and $\Omega_j = q_j B_0 / (m_j c)$. The plus and minus sign in the denominator of (5) refers to right and left hand polarization, respectively. After substitution of (4) into (5) we obtain the dispersion relation for the right and left hand polarized waves [see, for example, Scharer and Triefelpiece, 1967; Sentman et al., 1981]:

$$\begin{pmatrix} D_R \\ D_L \end{pmatrix} = \omega^2 - k_{\parallel}^2 c^2 + \sum_j \omega_{pj}^2 [\xi_j Z(\xi_j^{\pm}) + A_j Z'(\xi_j^{\pm}) / 2] = 0$$

$$\xi_j = \frac{\omega - k_{\parallel} v_{oj}}{k_{\parallel} \alpha_{\parallel j}}, \quad \xi_j^{\pm} = \xi_j \pm \frac{\Omega_j}{k_{\parallel} \alpha_{\parallel j}} \quad (6)$$

$A_j = 1 - \alpha_{\perp j}^2 / \alpha_{\parallel j}^2$ is the anisotropy, and $Z(\xi)$ and $Z'(\xi)$ are the plasma dispersion function and its derivative with respect to ξ [Fried and Conte, 1961].

To apply this formalism to the observations, we first estimate the plasma frame frequency and wave number using the Doppler shift equation together with the assumption that $\omega \ll \Omega_p$. The eigenvalue analysis provides both θ and the angle between \vec{k} and \vec{v}_{sw} . Because the rest frame polarization is known from the magnetic helicity spectrum, there are only two possibilities to consider, viz., whether the instability is resonant or nonresonant. We have investigated both possibilities for each interval.

The overall results of this instability analysis can be summarized in a general way before presenting the detailed computations below. The cold plasma, resonant instability ($\omega - k_{\parallel} v_{ob} + \Omega_p = 0$) was recently discussed by Goldstein et al. [1983]. For parallel propagation, there is only one unstable mode, viz., the right-hand fast mode, in which the beam velocity and wave phase velocity are parallel. In addition, there is a nonresonant instability, also right-hand, for which the beam and wave propagate antiparallel [see, e.g., Sentman, et al., 1981; Gary et al., 1984]. When the background plasma has a finite temperature, two new instabilities appear that are left hand polarized. First, there is a resonant instability ($\omega - k_{\parallel} v_{ob} - \Omega_p = 0$) that grows only if $A_b > 1$. In this case the beam velocity and wave phase velocity are antiparallel. Finally, there is a nonresonant left-hand instability (with the beam and wave propagating parallel) that can grow if the beam temperature is sufficiently large. A_b can be zero for this mode.

January 29, 1978 -- Upstream

The fluctuations in the upstream region of the January 29 shock were left-hand polarized in the range 0.025 - 0.07 Hz and were propagating parallel to the magnetic field, away from the reverse shock (into the upstream region).

The waves must be Doppler shifted "down" to $\omega' = \omega - \vec{k} \cdot \vec{V}_{sw}$ where ω' is the wave frequency as measured in the spacecraft frame in radians/s. By combining this with (6), we can determine the frequency of the wave in the solar wind frame, its phase velocity, its wavelength and the resonant velocity of the particles for our observations.

The plasma parameters for the background plasma, estimated from the Voyager data, are summarized in Table 1. Unstable roots of (6) were found under the assumption that the interaction was either resonant or non-resonant. The beam parameters used in the calculation of the wave characteristics were determined by requiring both that $\omega < \Omega_p$ and that the wavelengths and frequencies were in the observed range with the maximum growth rate occurring inside this range.

First consider the resonant interaction. Note that for this to be the physical mechanism for excitation of the observed waves, the beam will have to be propagating toward the shock front. Thus, we expect that this is not a likely scenario, but it is instructive to explore the range of physical parameters required to excite this mode. The unstable waves are found to have frequencies $(2.9 - 6.3) \times 10^{-3}$ Hz and wavelengths between $(4.82 - 13.7) \times 10^8$ cm. The maximum normalized growth rate (γ/Ω_p) for the resonant interaction is 2.34×10^{-2} at a wavelength of 7.13×10^8 cm and $\omega = 3.09 \times 10^{-2}$ rad/s. The average gyrofrequency for this event is 2.04×10^{-2} Hz (Table 1). Note, from Table 1, that this instability requires a very large ion beam thermal anisotropy (≈ 5) and a beam velocity of $V_{ob} = -41.25$ km/s (toward the shock).

In the case of the nonresonant interaction the unstable waves and beam will both be propagating away from the shock, which would appear to be a more reasonable situation than the geometry of the resonant interaction. The unstable waves are in the range of $(2.7 - 6.2) \times 10^{-3}$ Hz with similar wave-

lengths as for the resonant interaction. The maximum normalized growth rate for the non-resonant interaction is 2.68×10^{-3} at a wavelength of 6.56×10^8 cm and frequency $\omega = 3.2 \times 10^{-2}$ rad/s. For this instability, a hot isotropic "diffuse" proton population of about 222 eV streaming away of the shock at a velocity of $V_{ob} = 103$ km/s is required, which is just barely sufficient for the beam to propagate back upstream. This instability is insensitive to the value of A_b .

Recently, Hoppe and Russell [1983] have reported evidence for left-hand Alfvén wave fluctuations in the earth's foreshock region from ISEE-1 and 2 data. They concluded that the Alfvén mode could have been excited only by a diffuse population and not by a resonant beam interaction. Goldstein et al. [1983] argued that this was not necessary, because for oblique propagation the left-hand Alfvén mode can be resonantly excited. The situation that we have here is complementary in that we find that with a sufficient beam anisotropy amplification of left hand Alfvén waves is possible as anticipated by Hoppe and Russell [1983].

January 29, 1978 -- Downstream

A similar analysis has been performed in the downstream interval of the January 29 event for the observed frequency range of 0.01 - 0.015 Hz. During this interval left-hand waves are propagating parallel to the magnetic field toward the reverse shock. Thus, the frequency in the spacecraft frame must be Doppler shifted "down" by $\omega' = \omega - \vec{k} \cdot \vec{V}_{sw}$. Table 2 shows some of the results obtained assuming either a resonant and a nonresonant interaction.

For the resonant interaction the unstable modes are in the range of $(1.1 - 2.0) \times 10^{-3}$ Hz with wavelengths in the range $(1.35 - 2.7) \times 10^9$ cm. The maximum normalized growth rate is 5.71×10^{-4} at a wavelength of 1.8×10^9 cm

and frequency $\omega = 9.45 \times 10^{-3}$ rad/s. The beam parameters used in this calculation were $A_b = 1.7$ and $V_{ob} = -184$ km/s.

Similarly, the unstable modes for the non-resonant interaction occurs in the range of $(1.3 - 2.4) \times 10^{-3}$ Hz for the same wavelengths as in the resonant case. The maximum normalized growth rate for this interaction is 5.36×10^{-3} at a wavelength of 1.67×10^9 cm and frequency $\omega = 2.0 \times 10^{-3}$ rad/s. For this particular event the resonant interaction is much more probable because the ions are streaming away from the shock (into the downstream region) with modest anisotropies that are actually typical of the ambient solar wind.

At higher frequencies (Figure 6a), (0.05 - 0.2) Hz we found field aligned right-hand polarized waves. In the absence of cross helicity data in this frequency range, we shall assume that we are dealing with fast mode MHD waves propagating toward the shock (and the Sun). The dispersion relation is then given by (6) using the plus sign for right-hand waves. Since the solar wind is convecting away from the Sun, the waves observed at the spacecraft position must again be Doppler shifted "down". The instability analysis indicates that in the plasma frame ω extended from frequencies below the ion gyrofrequency to frequencies above it. This suggests that these waves may be right-hand ion cyclotron waves propagating nearly parallel to the magnetic field. These modes have been observed near interplanetary shocks by Tsurutani et al. [1983].

February 3, 1978

In this case the fluctuations were right-hand with frequencies in the range (0.025 - 0.17) Hz (in the spacecraft frame) propagating nearly anti-parallel to the magnetic field away from the forward shock (into the upstream

region). Similarly the wave characteristics in the plasma frame have also been calculated, using the dispersion relation (6) (with the plus sign for right hand waves) and the Doppler shift $\omega' = \omega + \vec{k} \cdot \vec{V}_{sw}$. Table 3 contains some results for the beam parameters that best fit the observations for both the resonant and nonresonant wave-particle interactions. In the resonant case, the wave frequencies in the plasma frame are about $(4.4 - 26) \times 10^{-3}$ Hz, with wavelengths between $(2.19 - 9.51) \times 10^8$ cm. The maximum normalized growth rate (γ/Ω_p) for resonant interaction occurred at 3.49×10^{-2} at a wavelength of 3.42×10^8 cm and frequency $\omega = 9.35 \times 10^{-2}$ rad/s. These modes can be excited by a proton beam streaming away from the shock (into the upstream region) with a thermal spread of about 38 ev and beam speed of -150 km/s (Table 3).

Excitation of the nonresonant mode requires an energetic proton beam propagating back toward the shock (and the sun). This is a very unlikely situation, and we further find that a very high beam speed of 557 km/s is required. The frequencies in the plasma frame of these unstable modes are between $(1.65 - 13.0) \times 10^{-3}$ Hz for the same wavelengths obtained in the resonant case and the maximum normalized growth rate for this case is 2.62×10^{-1} at a wavelength of 3.57×10^8 cm and $\omega = 4.0 \times 10^{-2}$ rad/s.

4. Discussion and Summary

We have presented three examples of low frequency waves associated with interplanetary shocks; a quasi-parallel forward shock and a reverse shocks. Two MHD modes have been identified. The first is a fast mode with characteristic frequencies in the range of 0.025 - 0.17 Hz (in the spacecraft frame). This mode is right-hand elliptically polarized propagating along the magnetic field. The second is an Alfvén mode with characteristic frequencies in the

range of 0.025 - 0.07 Hz (in the spacecraft frame). This mode is left-hand polarized and propagates within a few degrees of the magnetic field. The magnetic power spectra observed in the vicinity of these shocks are much steeper at high frequencies than is characteristic of either the ambient solar wind and or planetary shocks.

The analysis we have presented describes some of the basic properties of waves in the vicinity of interplanetary shocks. Our observations are consistent with either a resonant or nonresonant electromagnetic ion beam instability. In two of the three situations, the February 3, 1978, and the downstream side of the January 29, 1978 shocks, the geometry may be favorable for detecting the reflected proton distributions in the plasma data. This effort will be reported in a subsequent paper.

In spite of the limitations of the linear theory, and in spite of the many assumptions and limitations of our theoretical treatment, the electromagnetic ion beam instability appears capable of accounting for the major features of the observations. Similar conclusions have been reached in connection with planetary bow shocks by Barnes [1970], Gary et al. [1982], Lee [1982, 1983] and Goldstein et al. [1983], among others, and by Tsurutani et al. [1983] in their analysis of interplanetary shocks.

Acknowledgments. We thank H. S. Bridge and N. F. Ness, principal investigators of the Voyager plasma and magnetic field experiments respectively, for permission to use the plasma and magnetic field data, and W. H. Matthaeus, J. D. Scudder, L. F. Burlaga, D. H. Fairfield, and M. A. Lee for many stimulating discussions. H. K. Wong provided invaluable assistance with the instability calculations. E. Sittler is thanked for making available the electron data. We also wish to acknowledge the support of members of the Information Analysis and Display Branch at GSFC.

References

- Acuña, M. H., L. F. Burlaga, R. P. Lepping, and N. F. Ness, Initial results from the Voyagers 1, 2 magnetic field experiments, Solar Wind 4, IPAE Report#W-110-81-31, H. Rosenbauer, Ed., 1981.
- Barnes, A. Theory of generation of bow-shock-associated hydromagnetic waves in the upstream interplanetary medium, Cosmic Electrody., 1, 90, 1970.
- Barnes, A., and J. V. Hollweg, Large-amplitude hydromagnetic waves, J. Geophys. Res., 79, 2302, 1974.
- Batchelor, G. K., Theory of Homogeneous Turbulence, Cambridge University Press, New York, 1970.
- Behannon, K. W., M. H. Acuña, L. F. Burlaga, R. P. Lepping, N. F. Ness, and F. M. Neubauer, Magnetic field experiment for Voyagers 1 and 2 Spac. Sci. Rev., 21, 235, 1977.
- Bridge, H. S., J. W. Belcher, R. J. Butler, A. J. Lazarus, A. M. Mavretic, J. D. Sullivan, G. L. Siscoe, and V. M. Vasyliunas, The plasma experiment on the 1977 Voyager mission, Spac. Sci. Rev., 21, 259, 1977.
- Derby, N. F., Modulational instability of finite-amplitude circularly polarized Alfvén waves, Astrophys. J., 224, 1013, 1978.
- Fairfield, D. H., Bow-shock associated ~~waves~~ waves observed in the far upstream interplanetary medium, J. Geophys. Res., 74, 3541, 1969.
- Fairfield, D. H., Whistler waves observed upstream from collisionless shocks, J. Geophys. Res., 79, 1368, 1974.
- Fried, B. D. and S. D. Conte, The Plasma Dispersion Function, Academic Press, New York, 1961.
- Gary, S. P., J. T. Gosling, and D. W. Forslund, The electromagnetic ion beam instability upstream of the earth's bow shock, J. Geophys. Res., 86, 6691, 1981.

- Goldstein, M. L., An instability of finite amplitude circularly polarized Alfvén waves, Astrophys. J., 219, 700, 1978.
- Goldstein, M. L., C. W. Smith, and W. H. Matthaeus, Large amplitude MHD waves upstream of the Jovian Bow shock, J. Geophys. Res., in press, 1983.
- Hollweg, J. V., Density fluctuations driven by Alfvén waves, J. Geophys. Res., 76, 5155, 1971.
- Hoppe, M. M. and C. T. Russell, Plasma rest frame frequencies and polarizations of the low frequency upstream waves: ISEE-1 and -2 observations, J. Geophys. Res., submitted, 1983.
- Jackson, J. D. Classical Electrodynamics, John Wiley and Sons, 1962.
- Jokipii, J. R. and P. J. Coleman, Cosmic ray diffusion tensor and its variation observed with Mariner 4, J. Geophys. Res., 73, 5495, 1968.
- Kraichnan, R. H., Inertial range spectrum in hydromagnetic turbulence, Phys. Fluids, 8, 1385, 1965.
- Lashmore-Davies, C. N., Modulational instability of a finite amplitude Alfvén wave, Phys. Fluids, 19, 587, 1976.
- Lee, M. A., Coupled hydromagnetic wave excitation and ion acceleration upstream of the earth's bow shock, J. Geophys. Res., 87, 5063, 1982.
- Lee, M. A., The association of energetic particles and shocks in the heliosphere, Rev. Geophys. Spac. Phys., 21, 324, 1983.
- Lepping, R. P. and P. D. Argentiero, Single spacecraft method of estimating shock normals, J. Geophys. Res., 76, 4349, 1971.
- Matthaeus, W. H. and M. L. Goldstein, Measurements of the rugged invariants of magnetohydrodynamic turbulence in the solar wind, J. Geophys. Res., 87, 6011, 1982.
- Matthaeus, W. H., M. L. Goldstein, and C. W. Smith, Evaluation of magnetic helicity in homogeneous turbulence, Phys. Rev. Lett., 48, 1256, 1982.

- Moffatt, H. K., Magnetic Field Generation In Electrically Conducting Fluids, Cambridge University Press, 1978.
- Montgomery, D. C. and D. A. Tidman, Plasma Kinetic Theory, p. 146, Mc. Graw-Hill Co., New York, 1964.
- Russell, C. T., D. D. Childers, and P. J. Coleman, OGO-5 observations of upstream waves in the interplanetary medium: Discrete wave packets, J. Geophys. Res., 76, 845, 1971.
- Sakai, J., and B. U. Ö. Sonnerup, Modulational instability of finite amplitude dispersive Alfvén waves, J. Geophys. Res., in press, 1983.
- Scharer, J. E. and A. W. Trielpiece, Cyclotron wave instabilities in a plasma, Phys. Fluids, 10, 591, 1967.
- Scudder, J. D., L. F. Burlaga, and E. W. Greenstadt, Scale lengths in quasi-parallel shocks, to be submitted to GRL, 1983.
- Sentman, D. D., J. P. Edmiston, and L. A. Frank, Instabilities of low frequency, parallel propagating electromagnetic waves in the earth's fore-shock region, J. Geophys. Res., 86, 7487, 1981.
- Smith, C. W., M. L. Goldstein, and W. H. Matthaeus, Turbulence analysis of the Jovian upstream 'wave' phenomenon, J. Geophys. Res., 88, 5581, 1983.
- Smith, C. W., M. L. Goldstein, and C. T. Russell, Observations of harmonic ion-cyclotron resonances upstream of earth, J. Geophys. Res., submitted, 1984.
- Taylor, G. I., Statistical theory of turbulence, Proc. R. Soc. London, Ser. A, 151, 421, 1935.
- Taylor, G. I., The spectrum of turbulence, Proc. R. Soc. London, Ser. A, 164, 476, 1938.
- Tsurutani, B., E. J. Smith, and D. E. Jones, Waves observed upstream of interplanetary shocks, J. Geophys. Res., 88, 5645, 1983.

Figure Captions

Figure 1. Voyager 2 magnetic field and plasma data of a reverse quasi-parallel shock occurring at 0918:17 UT on January 29, 1978 at about 2.16 AU.

Figure 2. Trace of the magnetic energy spectrum from the upstream region (0919:10-1000 UT) for the January 29 event. The data used are 1.92 s averages and the spectrum contains 26 degrees of freedom.

Figure 3. a. The normalized reduced magnetic helicity spectrum σ_m after Matthaeus and Goldstein [1982].

b. The degree of polarization D as obtained from an eigenvalue analysis of this interval.

c. The ellipticity ϵ as calculated from the eigenvalue analysis.

d. The cosine of the angle θ between \vec{k} and \vec{B}_0 as obtained from the eigenvalue analysis imposing the requirement that \vec{k} has a positive projection in the +R direction.

Figure 4. a. The normalized cross-helicity spectrum σ_c after Matthaeus and Goldstein [1982]. The data used are 12 s averages and the spectrum contains 14 degrees of freedom.

b. The correlation between $|\vec{B}|$ and ρ .

c. The Alfvén ratio $r_A = E_v(k)/E_b(k)$ where $E_v(k)$ and $E_b(k)$ are the reduced spectra of kinetic and magnetic energy respectively.

Figure 5. The trace of the magnetic power spectral density for the downstream interval (0800:45-0914:39 UT) on January 29 event. This spectrum has 26 degrees of freedom.

Figure 6. Plotted in a-d are σ_m , D , ϵ , and $\cos\theta$, respectively, for the downstream region.

Figure 7. Plotted in a-c are σ_c , the $|\vec{B}|-\rho$ correlation, and the Alfvén ratio r_A respectively, for the downstream region.

Figure 8. Voyager 1 magnetic field and plasma data of a quasi-parallel forward shock (in formation) occurring at 1928 UT on February 3, 1978 at about 2.25 AU.

Figure 9. Trace of the magnetic energy spectrum for the upstream region (1850-1926 UT) of the February 3 event.

Figure 10. The same as Fig. 6, but for the upstream region of the February 3 event.

Figure 11. The same as Fig. 7, but for the upstream region of the February 3 event.

Figure 12. a. The density spectrum for the February 3 event containing 14 degrees of freedom.

b. The magnetic field magnitude spectrum.

Table 1. Plasma parameters for January 29, 1978 (Upstream)

Left-hand, Nonresonant Instability

	Background electrons		Background ions		Ion beam	
	Resonant	Nonresonant	Resonant	Nonresonant	Resonant	Nonresonant
n_j (#/cm ³)	.50	.50	0.47	0.47	0.005	0.005
$k_B T_{\parallel j}$ (eV)	6.15	6.15	1.47	1.47	26.65	222.
$k_B T_{\perp j}$ (eV)	6.15	6.15	1.47	1.47	133.26	222.
V_{oj} (km/s)	0.0	0.0	0.42	-1.04	-42.25	103.

The Alfvén speed is 4.12×10^6 , $V_{sw} = 3.66 \times 10^7$, $\Omega_p = 2.04 \times 10^{-2}$

Table 2. Plasma parameters for January 29, 1978 (Downstream)

Left-hand, Resonant Instability

	Background electrons		Background ions		Ion beam	
	Resonant	Nonresonant	Resonant	Nonresonant	Resonant	Nonresonant
n_j (#/cm ³)	1.36	1.36	1.27	1.27	0.014	0.014
$k_B T_{\parallel j}$ (eV)	6.09	6.09	5.52	5.52	141.84	319.14
$k_B T_{\perp j}$ (eV)	6.09	6.09	5.52	5.52	248.22	319.14
V_{oj} (km/s)	0.0	0.0	1.86	0.93	-184.3	92.15

The Alfvén speed is 3.68×10^6 , $V_{sw} = 3.37 \times 10^7$, $\Omega_p = 3.01 \times 10^{-2}$

Table 3. Plasma parameters for February 3, 1978 (Upstream)

Right-hand, Resonant Instability

	Background electrons		Background ions		Ion beam	
	Resonant	Nonresonant	Resonant	Nonresonant	Resonant	Nonresonant
n_j (#/cm ³)	1.64	1.64	1.52	1.52	0.016	0.082
$k_B T_{\parallel j}$ (eV)	5.27	5.27	5.64	5.64	38.4	9.6
$k_B T_{\perp j}$ (eV)	5.27	5.27	5.64	5.64	38.4	9.6
V_{oj} (km/s)	0.0	0.0	1.52	-29.34	-150.	557.4

The Alfvén speed is 4.28×10^6 , $V_{sw} = 3.99 \times 10^7$, $\Omega_p = 3.84 \times 10^{-2}$

JANUARY 29, 1978

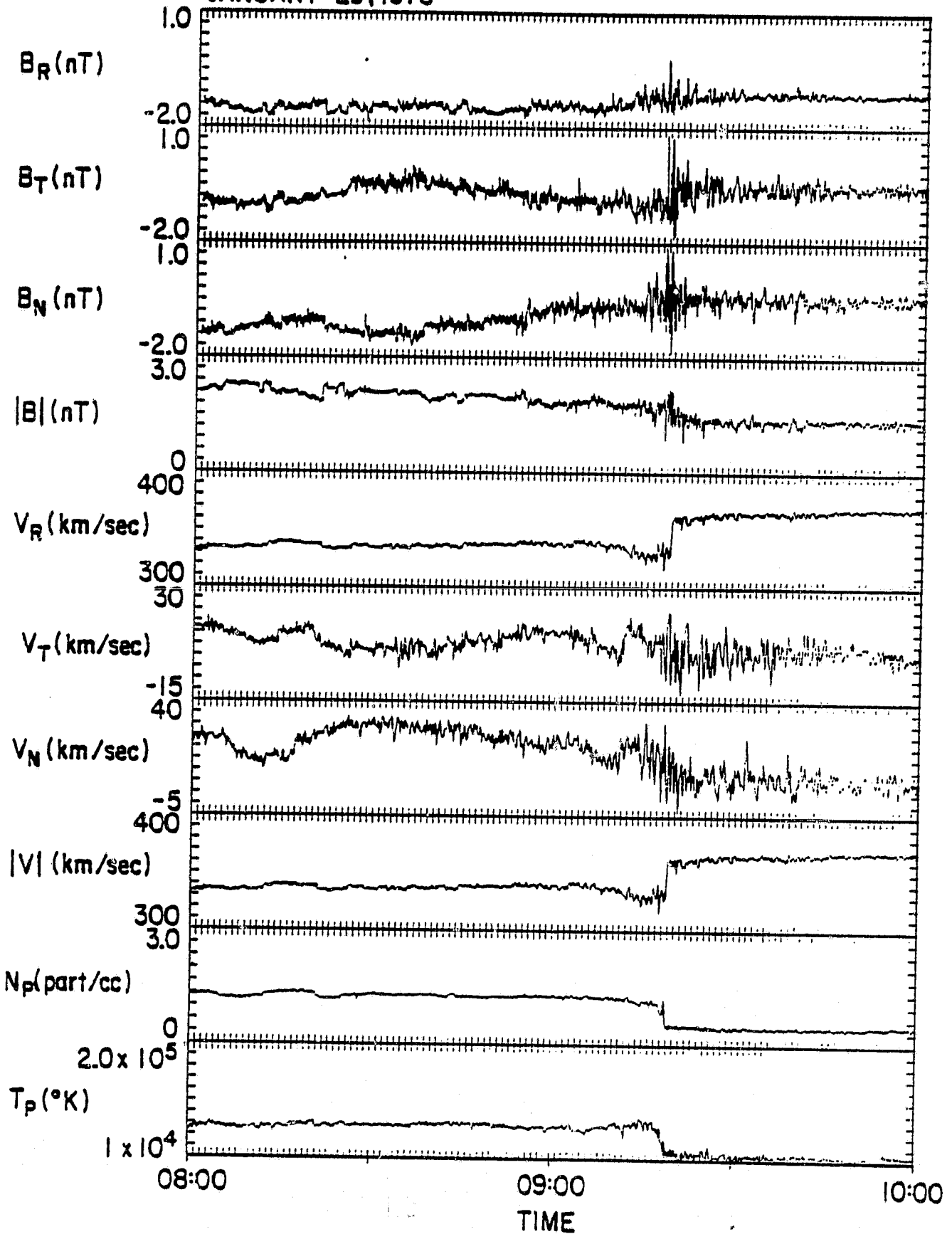


Figure 1

ORIGINAL PAGE IS
OF POOR QUALITY.

ORIGINAL PAGE IS
OF POOR QUALITY

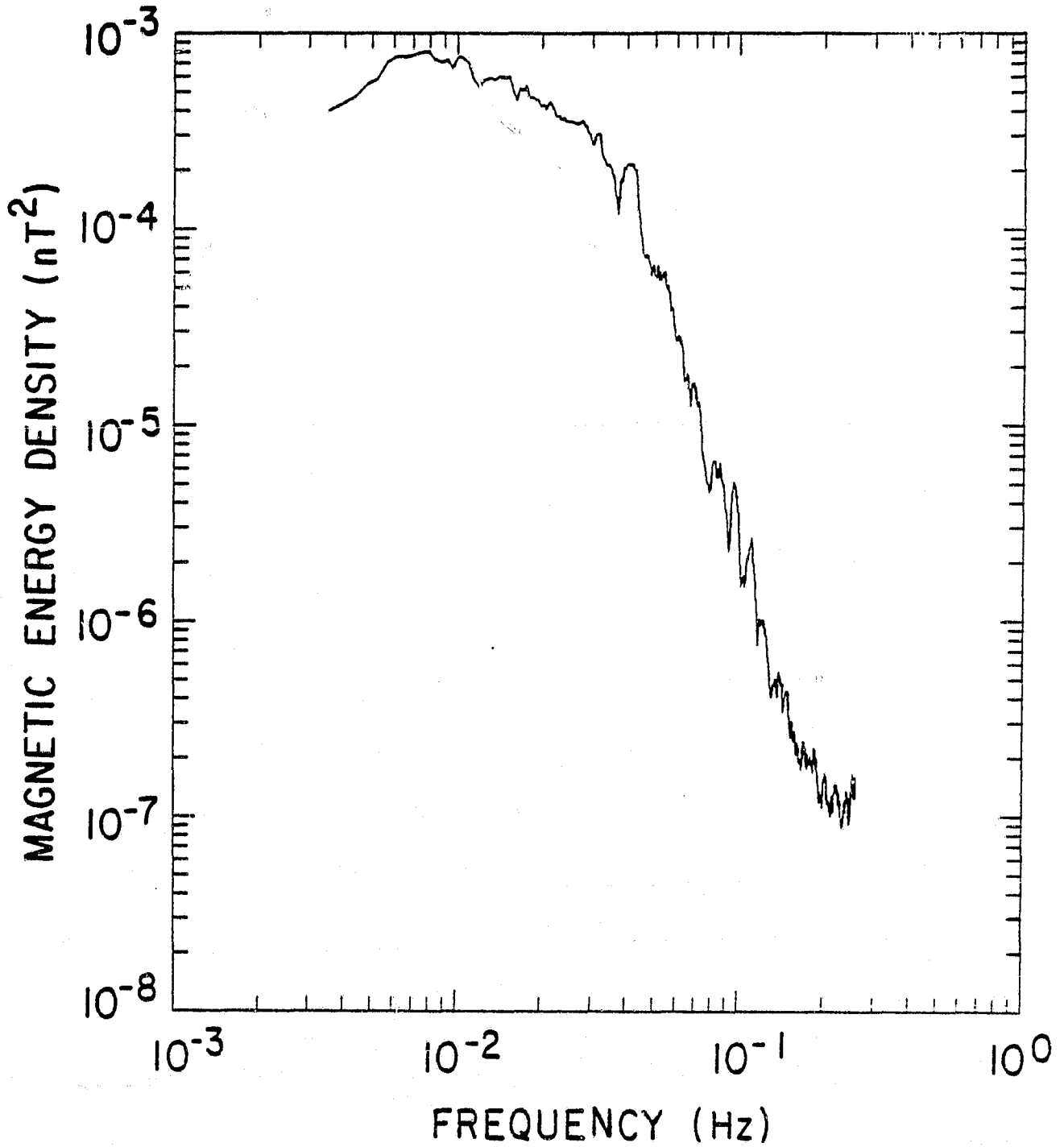


Figure 2

JANUARY 29, 1978 (UPSTREAM)

ORIGINAL PAGE IS
OF POOR QUALITY

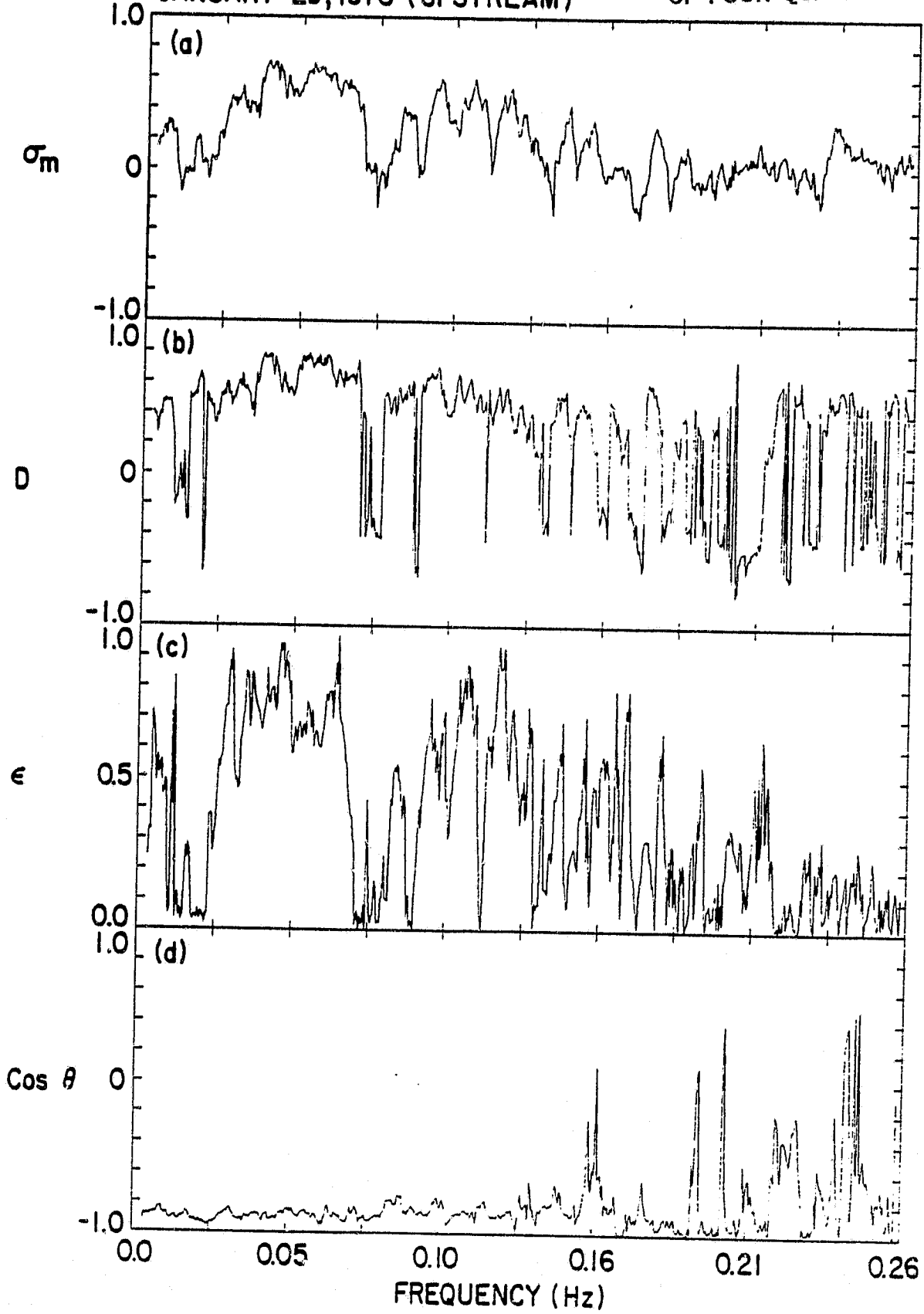


Figure 3

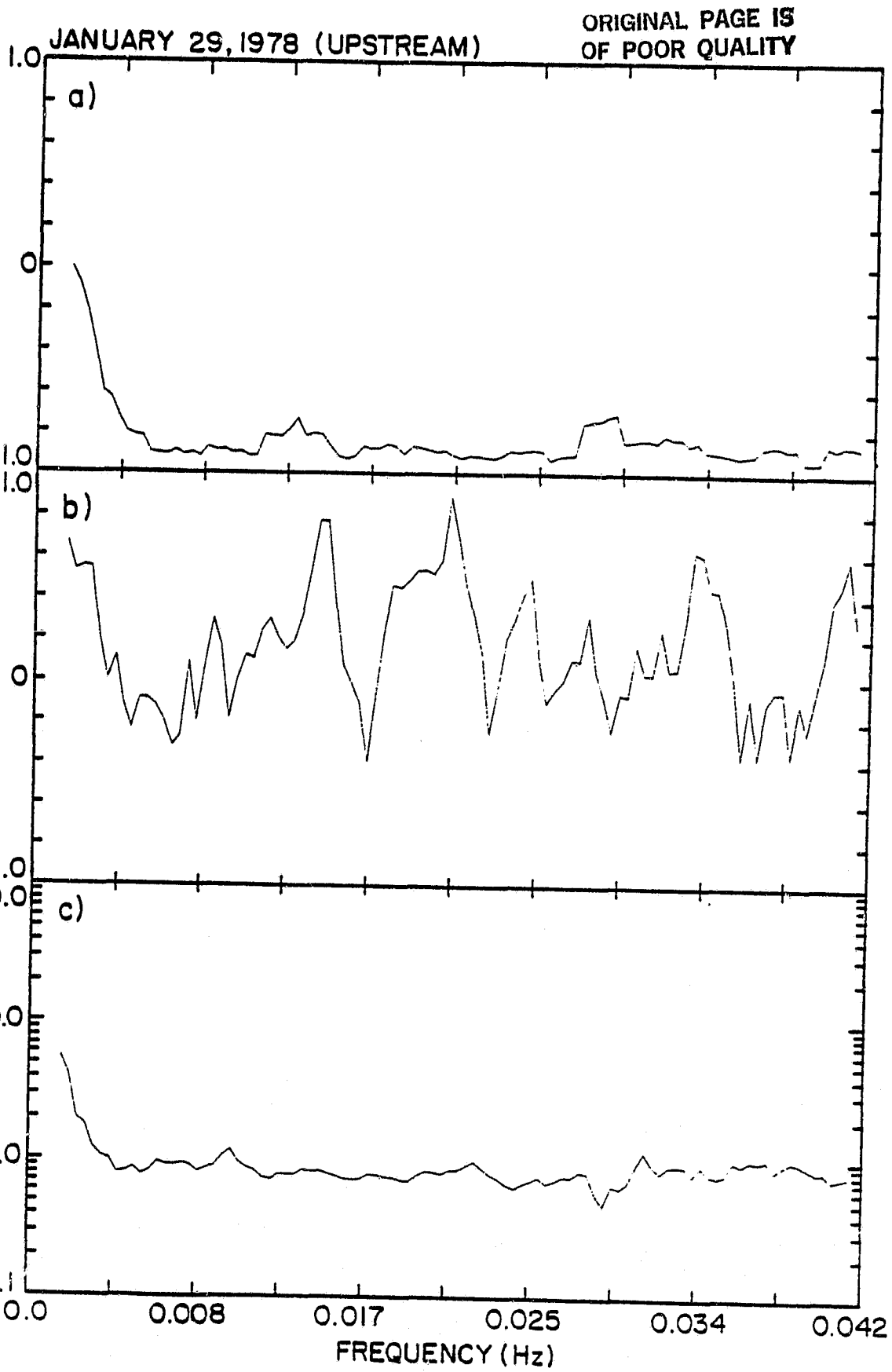


Figure 4

ORIGINAL PAGE 19
OF POOR QUALITY

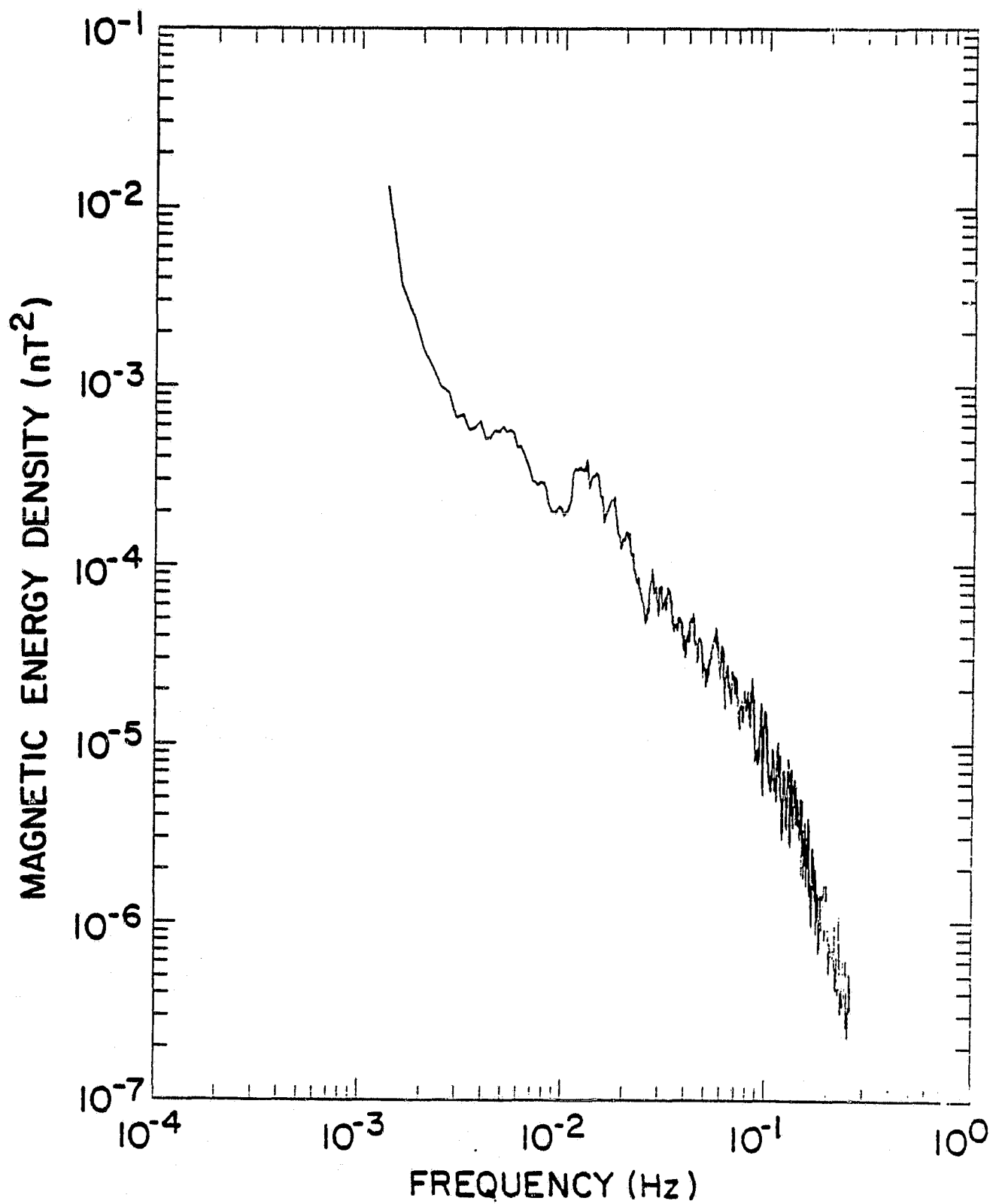


Figure 5

JANUARY 29, 1978 (DOWNSTREAM)

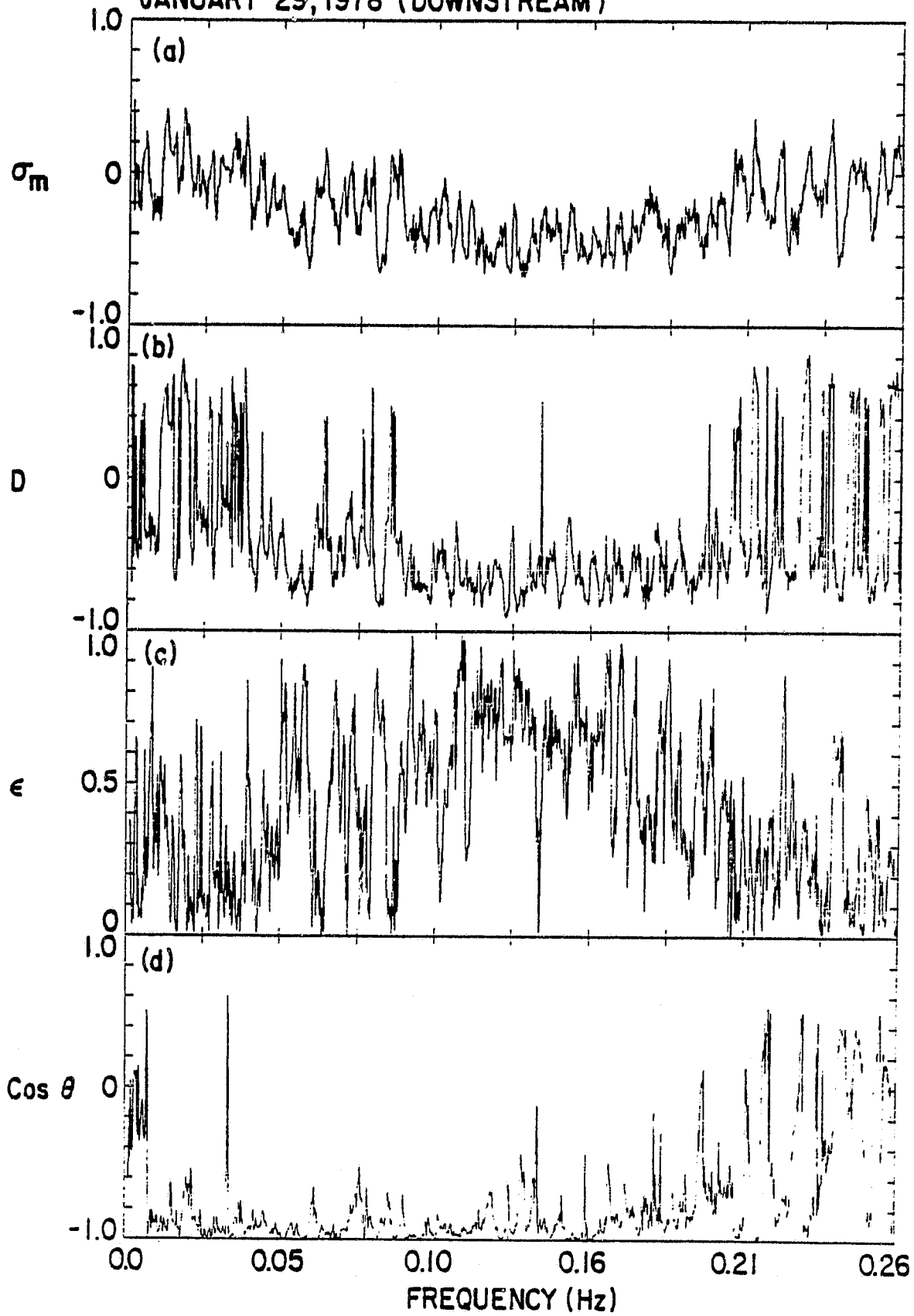


Figure 6

JANUARY 29, 1978 (DOWNSTREAM)

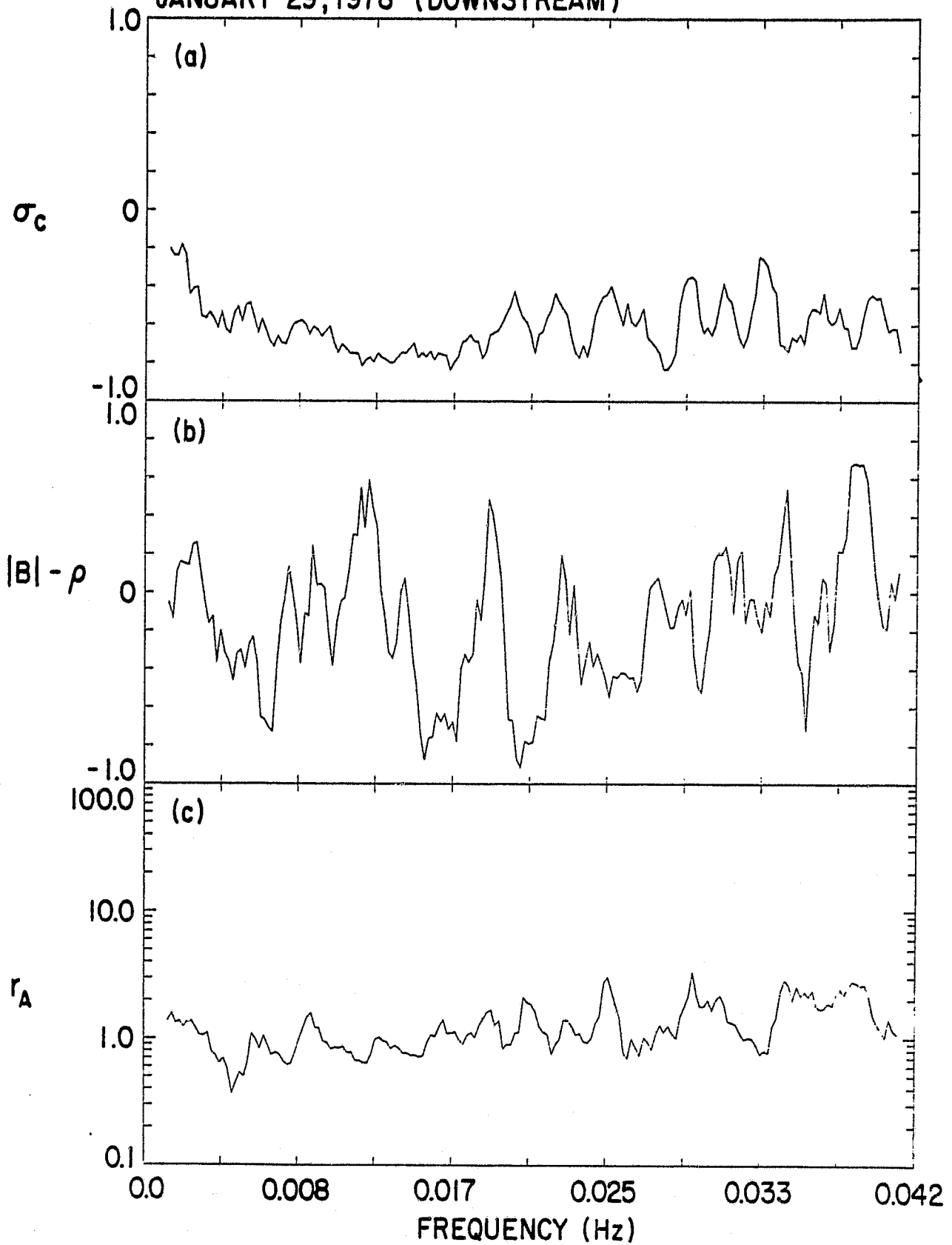


Figure 7

FEBRUARY 3, 1978

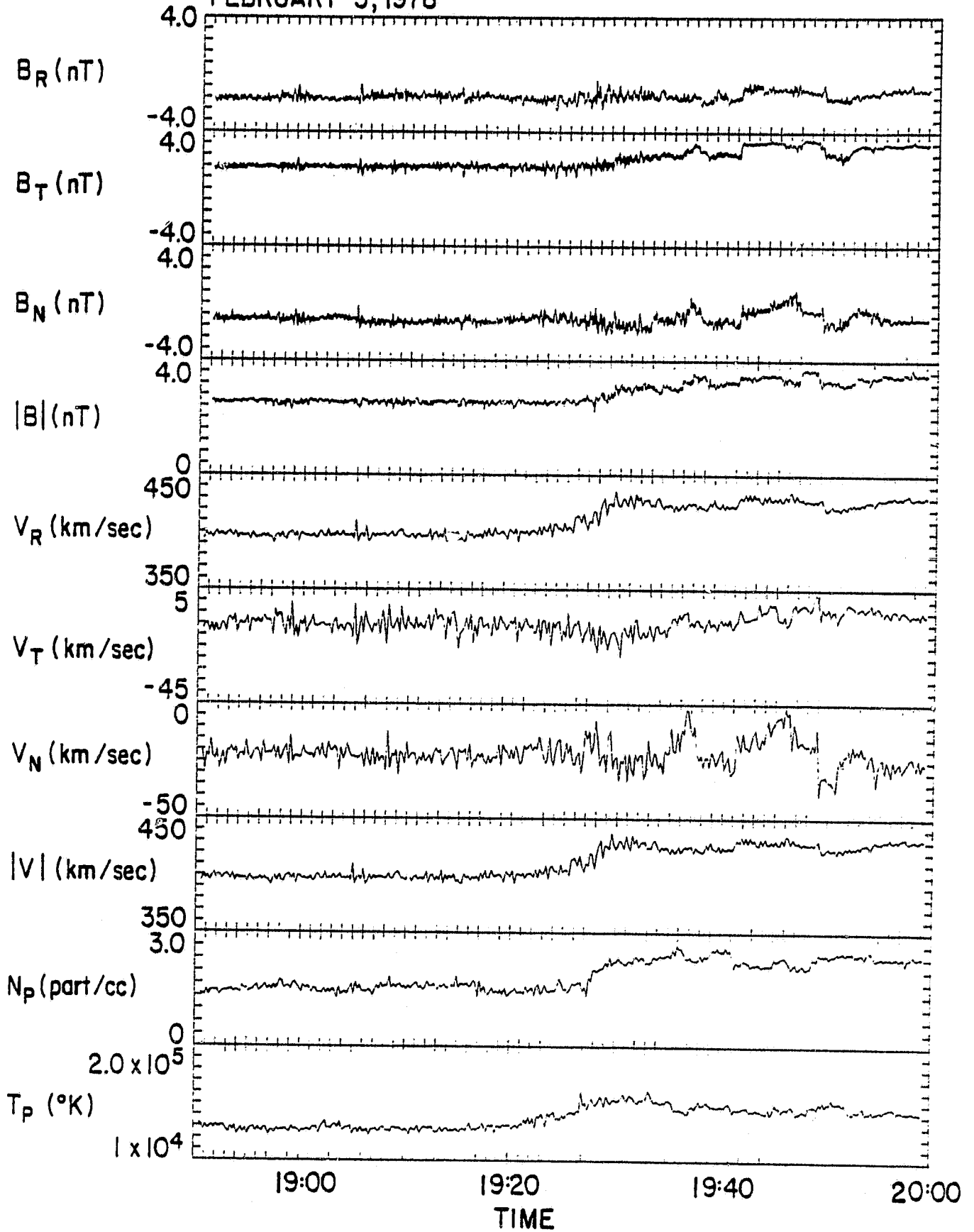


Figure 8

ORIGINAL PAGE 15
OF POOR QUALITY

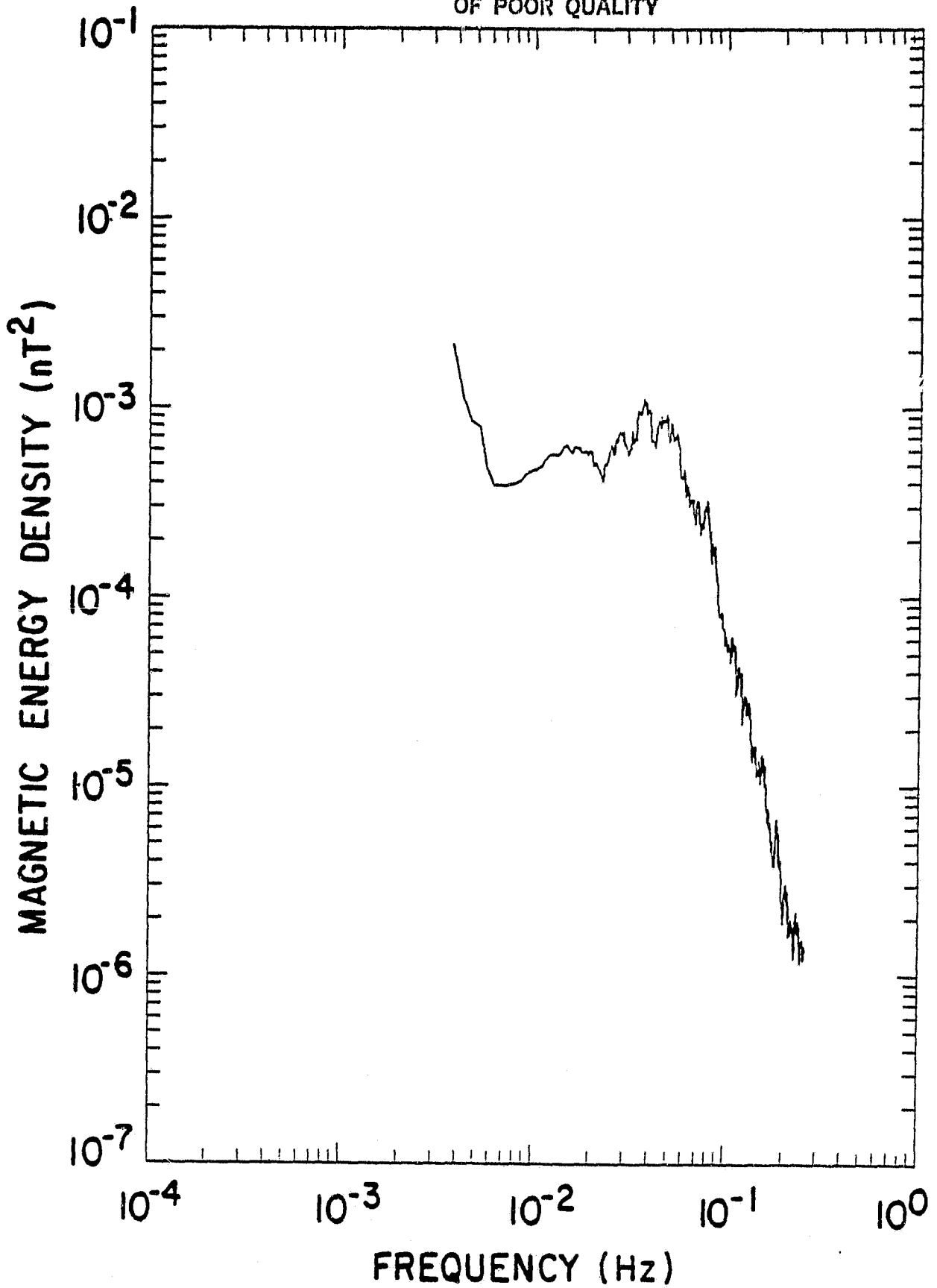


Figure 9

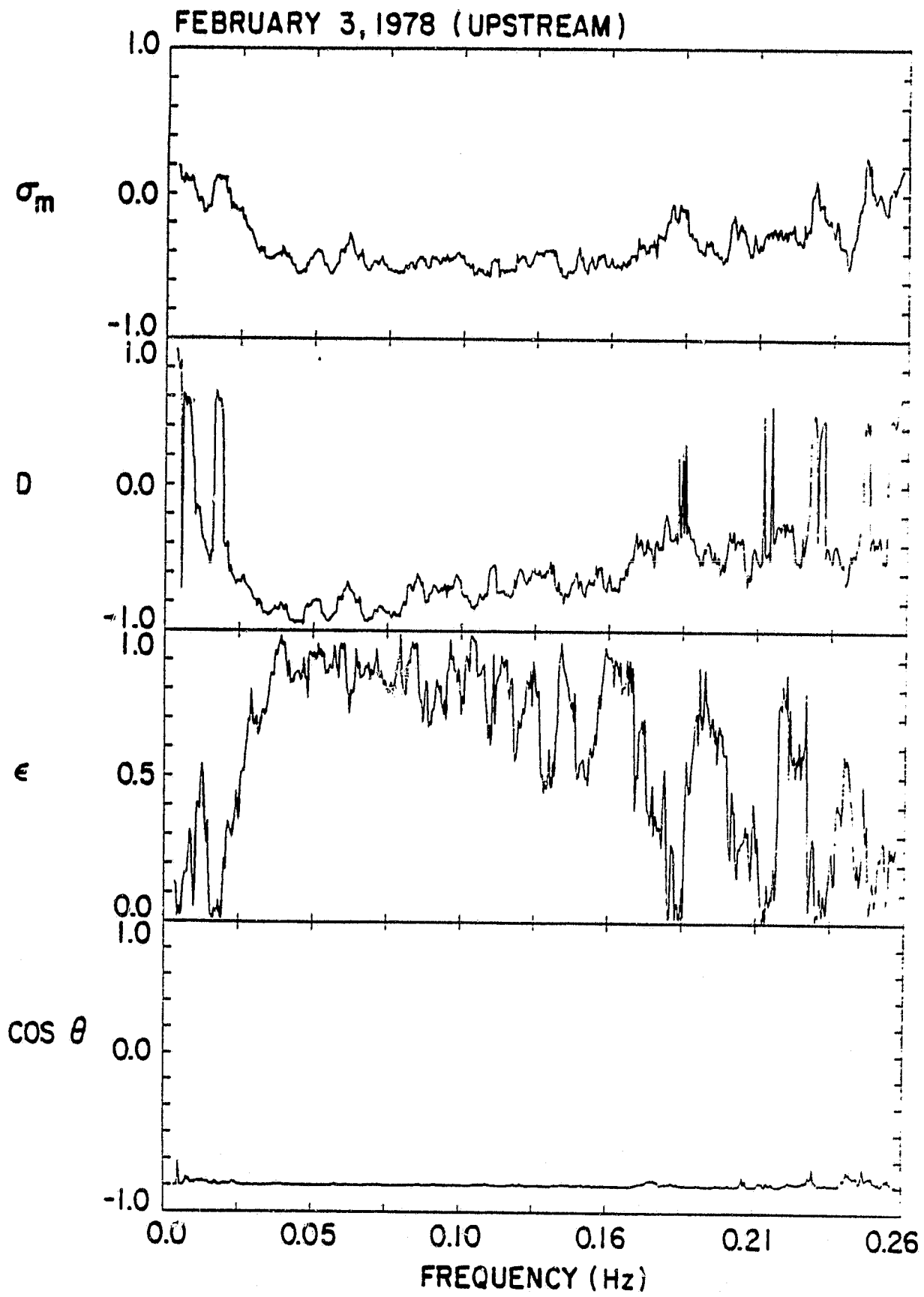


Figure 10

FEBRUARY 3, 1978 (UPSTREAM)

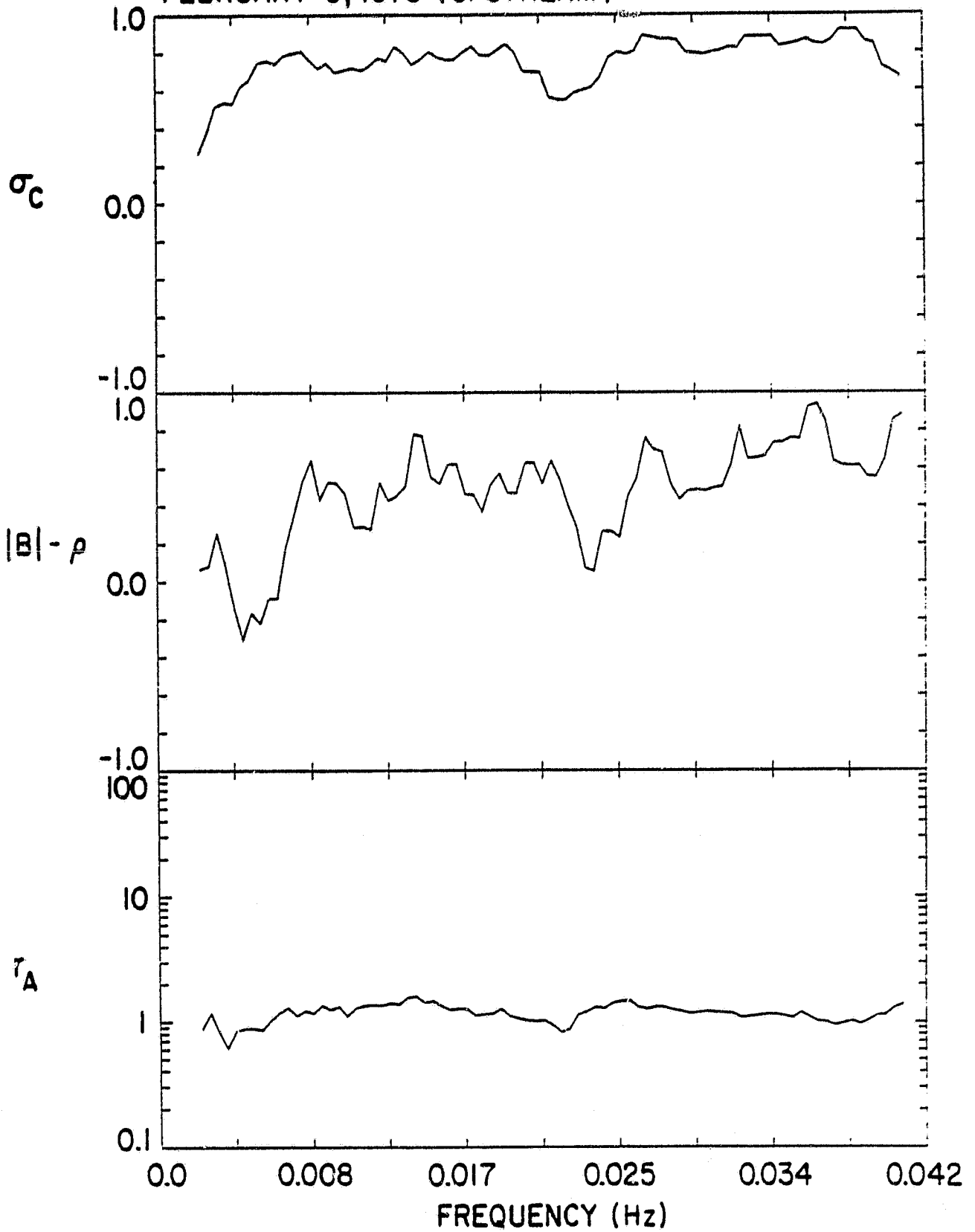


Figure 11

ORIGINAL PAGE IS
OF POOR QUALITY

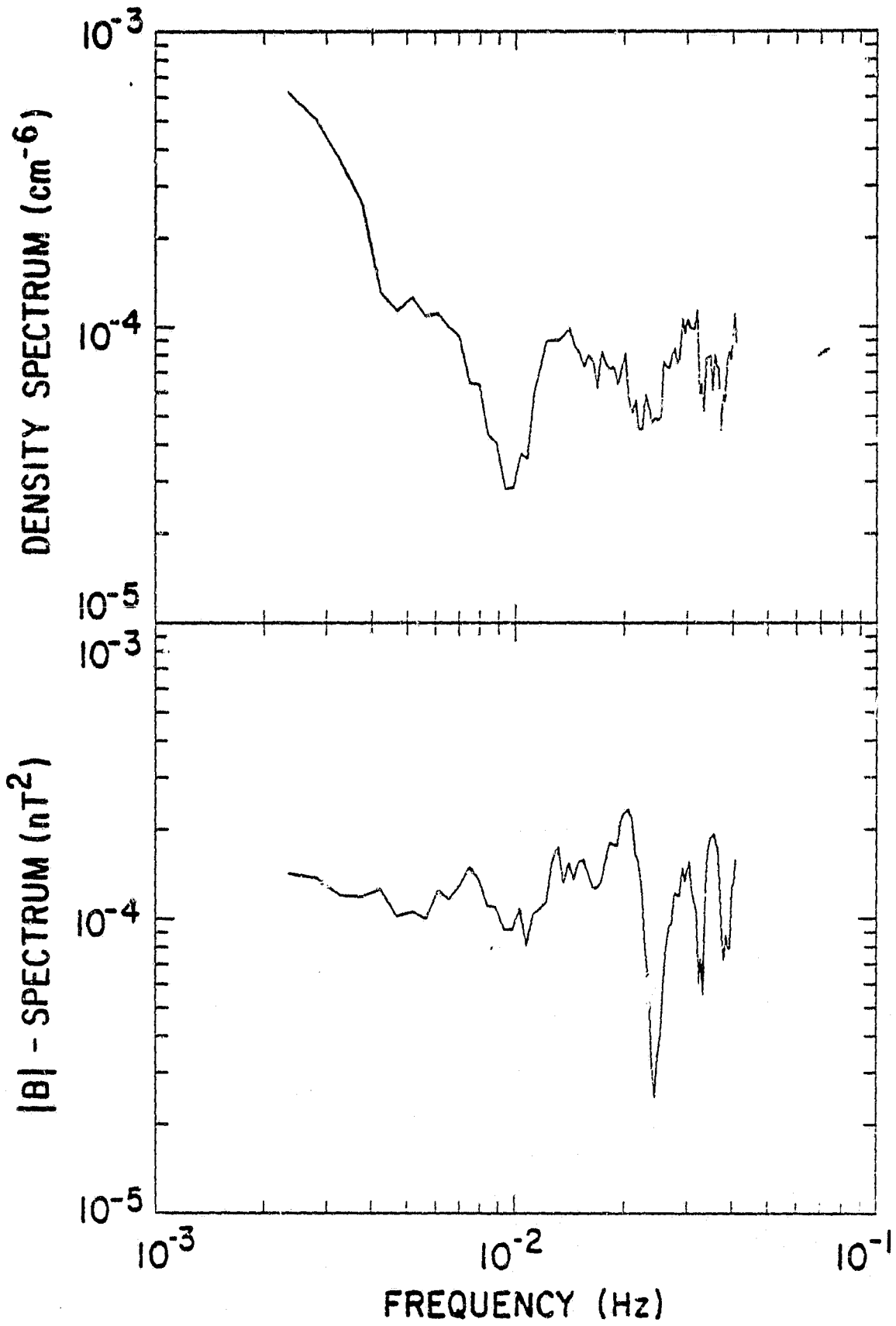


Figure 12